Journal of Neurochemistry

JOURNAL OF NEUROCHEMISTRY | 2012 | 122 | 147–161 doi: 10.1111/j.1471-4159.2012.07762.x

ORIGINAL ARTICLE

Receptor protein tyrosine phosphatase sigma regulates synapse structure, function and plasticity

Katherine E. Horn,*[,1] Bin Xu,*[,1] Delphine Gobert,* Bassam N. Hamam,† Katherine M. Thompson,* Chia-Lun Wu,‡ Jean-François Bouchard,* Noriko Uetani,‡ Ronald J. Racine,§ Michel L. Tremblay,‡ Edward S. Ruthazer,* C. Andrew Chapman† and Timothy E. Kennedy*

*Department of Neurology and Neurosurgery, Montreal Neurological Institute, McGill University, Montreal, Quebec, Canada

†Department of Psychology, Center for Studies in Behavioral Neurobiology, Concordia University, Montreal, Quebec, Canada

‡Goodman Cancer Centre and Department of Biochemistry, McGill University, Montreal, Quebec, Canada

§Department of Psychology, McMaster University, Ontario, Canada

Abstract

The mechanisms that regulate synapse formation and maintenance are incompletely understood. In particular, relatively few inhibitors of synapse formation have been identified. Receptor protein tyrosine phosphatase σ (RPTPσ), a transmembrane tyrosine phosphatase, is widely expressed by neurons in developing and mature mammalian brain, and functions as a receptor for chondroitin sulfate proteoglycans that inhibits axon regeneration following injury. In this study, we address RPTPσ function in the mature brain. We demonstrate increased axon collateral branching in the hippocampus of RPTPσ null mice during normal aging or following chemically induced seizure, indicating that RPTPσ maintains neural circuitry by inhibiting axonal branching. Previous studies demonstrated a role for pre-synaptic RPTPσ promoting synaptic differentiation during development; however, subcellular fractionation revealed enrichment of RPTPσ in post-synaptic densities. We report that neurons lacking RPTPσ have an increased density of pre-synaptic varicosities *in vitro* and increased dendritic spine density and length *in vivo*. RPTPσ knockouts exhibit an increased frequency of miniature excitatory post-synaptic currents, and greater paired-pulse facilitation, consistent with increased synapse density but reduced synaptic efficiency. Furthermore, RPTPσ nulls exhibit reduced long-term potentiation and enhanced novel object recognition memory. We conclude that RPTPσ limits synapse number and regulates synapse structure and function in the mature CNS.

Keywords: CSPG, LAR, LTP, RPTPσ, RPTPsigma.

J. Neurochem. (2012) **122**, 147–161.

Receptor protein tyrosine phosphatases (RPTPs) are a large family of transmembrane proteins implicated in axon growth and guidance (Chagnon *et al.* 2004; Tremblay 2009). The type IIa subfamily of RPTPs in mammals includes leukocyte common antigen-related (LAR), RPTPδ, and RPTPσ. All three family members are expressed in the developing and mature mammalian CNS: RPTPσ is widely expressed by neurons, while expression of LAR and RPTPδ is more restricted (Yan *et al.* 1993; Wang *et al.* 1995; Sommer *et al.* 1997; Schaapveld *et al.* 1998; Zhang *et al.* 1998). RPTPσ expression is not limited to the nervous system, and although RPTPσ knockout mice live to adulthood and are fertile, they exhibit multiple developmental deficiencies including

Received February 10, 2012; revised manuscript received March 22, 2012; accepted April 16, 2012.

Address correspondence and reprint requests to Timothy E. Kennedy, Centre for Neuronal Survival, Montreal Neurological Institute, McGill University, 3801 University Avenue, Montreal, Quebec, Canada H3A 2B4. Email: timothy.kennedy@mcgill.ca

[1]These authors contributed equally to this work.

Abbreviations used: ACSF, artificial CSF; AMPA, α-amino-3-hydroxy-5-methyl-4-isoxazolepropionic acid; AMPAR, AMPA receptor; CSPG, chondroitin sulfate proteoglycan; fEPSP, field excitatory post-synaptic potential; HSPG, heparin sulfate proteoglycan; KA, kainic acid; LAR, leukocyte common antigen-related; LTD, long-term depression; LTP, long-term potentiation; MAP-2, microtubule-associated protein 2; mEPSP, miniature excitatory post-synaptic current; NGL-3, netrin-G ligand 3; PSD, post-synaptic density; RPTP, receptor protein tyrosine phosphatase; VAMP2, vesicle-associated membrane protein 2.

retarded growth, elevated mortality rate, delayed peripheral nerve development, and altered development of the hypothalamus, olfactory bulb, and pituitary gland (Elchebly *et al.* 1999; Wallace *et al.* 1999). Studies of developmental synaptogenesis carried out *in vitro* have provided evidence that pre-synaptic LAR, RPTPδ and RPTPσ promote the differentiation of glutamatergic synapses through trans-synaptic interactions with post-synaptic netrin-G ligand 3 (NGL-3) and TrkC (Dunah *et al.* 2005; Stryker and Johnson 2007; Woo *et al.* 2009; Kwon *et al.* 2010; Takahashi *et al.* 2011).

Recent findings indicate that RPTPσ is a receptor for chondroitin sulfate proteoglycans (CSPGs), which are key components of glial scars that inhibit axon regeneration in the CNS following injury (Shen *et al.* 2009; Fry *et al.* 2010; Coles *et al.* 2011). Consistent with this, the absence of RPTPσ promotes axon regeneration in both the PNS and CNS (Thompson *et al.* 2003; Sapieha *et al.* 2005; Fry *et al.* 2010). Based on these findings, we hypothesized that RPTPσ expression in the intact adult nervous system may function to inhibit axon growth, sprouting, and synapse formation.

Investigating the distribution and function of RPTPσ in the CNS, we report that RPTPσ is enriched in synaptosomes and post-synaptic densities. Increased hippocampal mossy fiber axon sprouting was detected in RPTPσ null mice during aging and following chemically induced seizures, consistent with RPTPσ inhibiting axon growth and limiting synapse formation. RPTPσ knockouts also exhibited an increased density of pre-synaptic varicosities in neuronal cultures and increased dendritic spine density and spine length along CA1 pyramidal cell dendrites *in vivo*. In accordance with these findings, we detected an increase in the frequency of miniature post-synaptic α-amino-3-hydroxy-5-methyl-4-isoxazolepropionic acid (AMPA) currents, and an increase in paired-pulse facilitation in RPTPσ knockouts, consistent with increased synapse density but reduced synaptic efficiency. Mice deficient in RPTPδ are impaired in learning and memory tasks and exhibit enhanced long-term potentiation (LTP), a form of activity dependent plasticity (Uetani *et al.* 2000). In contrast to RPTPδ, we identified reduced LTP at hippocampal Schaffer collateral-CA1 synapses in RPTPσ null mice, and enhanced performance in a novel object recognition memory task. Our findings identify novel roles for RPTPσ regulating synapse structure and function, synaptic plasticity and learning and memory, and reveal diversity in the function of members of the LAR family of type IIa RPTPs at synapses.

Materials and methods

Animals

All procedures were performed in accordance with the *Canadian Council on Animal Care* guideline for the use of animals in research. Transgenic mice lacking RPTPσ were generated and bred in a Balb/C background as described (Elchebly *et al.* 1999). For subcellular fractionation, adult Long-Evans hooded rats (250 to 300g) were obtained from Charles River Canada (QC).

Subcellular fractionation and western blotting

Cortices from adult rats and postnatal day 14 (P14) rats were dissected and homogenized in ice cold homogenization buffer (0.32 M sucrose, 1 mM $NaHCO_3$, 1 mM $MgCl_2$, 0.5 mM $CaCl_2$, 2 μg/mL aprotinin, 2 μg/mL leupeptin, 1 μg/mL pepstatin) in a teflon-glass homogenizer. For subcellular fractionation, homogenates were fractionated by differential centrifugation as described (Cohen *et al.* 1977; Ueda *et al.* 1979; Carlin *et al.* 1980). Post-synaptic density fractionation of adult rat brain (Unstripped, 56004-2; Pel-Freez Biologicals, Rogers, AR, USA) was performed as described (Fallon *et al.* 2002). Protein concentration was quantified using the BCA kit (Pierce, Rockford, IL, USA). For fractionations and western blots, protein was separated using sodium dodecyl sulfate–polyacrylamide gel electrophoresis and transferred to a nitrocellulose membrane (Amersham Pharmacia Biotech, Piscataway, NJ, USA). Following blocking for 1 h at ~25°C in 5% milk Tris-buffered saline with Tween 20 (10 mM Tris pH 7.5, 100 mM NaCl, 0.1% Tween 20), membranes were incubated with mouse monoclonal anti-beta-tubulin III (1 : 500, T4026; Sigma-Aldrich, St. Louis, MO, USA), rabbit polyclonal anti-GluR2/3 (1 : 1000, AB1506; Chemicon, Temecula, CA, USA), rabbit polyclonal anti-LAR (1 : 500; Santa Cruz Biotechnology, Santa Cruz, CA, USA), mouse monoclonal anti-PSD95 (1 : 500; BD Pharmingen, San Jose, CA, USA); goat polyclonal anti-RPTPδ (1 : 500, K20; Santa Cruz) mouse monoclonal anti-RPTPσ (17G7.2; 1 : 500; Thompson *et al.* 2003), mouse monoclonal anti-synaptophysin (1 : 10 000, S 5768; Sigma-Aldrich), rabbit polyclonal anti-synaptotagmin I (8907, provided by P. De Camilli, Yale University, New Haven, CT, USA) or rabbit polyclonal anti-VAMP2 (vesicle-associated membrane protein 2, 1 : 1000; Chemicon) in blocking solution at 4°C overnight. Immunoreactivity was visualized using peroxidase-conjugated secondary antibodies (Jackson ImmunoResearch, West Grove, PA, USA) and Chemiluminescence Reagent Plus protein detection (NEN Life Science Products, Boston, MA, USA).

Kainic acid-induced status epilepticus, Timm staining, and histology

Prior to seizure induction, animals were injected with methyl scopolamine (1 mg/kg; i.p.) to prevent the peripheral autonomic effects of kainic acid. Adult RPTP$\sigma^{-/-}$ and RPTP$\sigma^{+/+}$ mice aged between 10 and 12 weeks received a single i.p. injection of kainic acid (KA) at a dose of 20 mg/kg. The development of behavioral seizures was monitored and graded by an observer blind to the experimental conditions according to the Racine Classification (Racine 1972): class 1, facial clonus; class 2, head nodding; class 3, unilateral forelimb clonus; class 4, rearing with bilateral forelimb clonus; and class 5, rearing and falling (loss of postural control). Once animals experienced status epilepticus (continuous behavioral seizures) for 2 h, seizures were terminated with a single dose of sodium pentobarbital of 20 mg/kg.

Four weeks following KA treatment, animals were perfused transcardiacally with sodium sulfide solution (8.9 g $Na_2S{\cdot}9H_2O$, 10.9 g sucrose, and 1.19 g $Na_2HPO_4{\cdot}H_2O$ per 100 ml dH_2O). Brains

were removed and immediately frozen in isopentane cooled to −40°C. Horizontal, serial, 40 μm sections were cut with a cryostat (Leica CM1850; Leica Microsystems Inc., Richmond Hill, ON, Canada). Alternate sections were stained using either a modified Timm staining method (Xu *et al.* 2004) for the analysis of Timm granule density, or Cresyl violet to determine the neuronal density in the hilar area.

Untreated young adults aged between 10 and 14 weeks, or aged adults between 14 to 16 months were perfused and processed as described above to evaluate the baseline level of Timm granule density in young and aged hippocampi. The Timm staining procedure selectively labels mossy fibers in the dentate gyrus and CA3 due to relatively high concentrations of Zn^{2+} present. Using an Axiovert 100 microscope (Carl Zeiss, Toronto, ON, Canada), digital images of hippocampus were captured from five horizontal sections 4.0, 4.7, 5.4, 6.1, and 6.8 mm ventral to bregma, and analyzed using Northern Eclipse software (Empix Imaging, Mississauga, ON, Canada). All images, including the fluorescence immunohistochemistry described below, were obtained and quantified by an observer blind to the experimental conditions using the same exposure time to allow comparison of measurements within an experiment.

Measurements were collected, including the optical density of Timm granules within the CA3c and CA3a subregions, and subjected to four-way repeated measures ANOVAs. To evaluate whether KA treatment induced neuronal damage in wild-type or RPTP$\sigma^{-/-}$ mice, the number of neurons located in the hilus was counted on five horizontal sections from mice that had received KA treatment and a three-way ANOVA (genotypes × sections × hemispheres) conducted.

Embryonic cortical neuron culture

Cultures of dispersed embryonic cortical neurons were prepared as described (Thompson *et al.* 2003). In brief, neocortices from RPTPσ null and wild-type E15 littermates were dissected in Hanks' balanced salt solution (Invitrogen, Burlington, ON, Canada). Diced tissue was treated with 0.25% trypsin (Invitrogen) in SMEM (Invitrogen) at 37°C for 25 min and washed in Neurobasal medium containing 10% heat-inactivated fetal bovine serum (Biomedia, QC, Canada), 2 mM glutamine, 100 units/mL penicillin, and 100 μg/mL streptomycin. Cells were plated at a density of 25 000 cells per poly-D-lysine (Sigma) pre-coated 12 mm glass coverslip (Carolina Biological Supply, Burlington, NC, USA).

Immunohistochemistry and image analysis

After 14 days *in vitro*, cortical cultures were fixed with 4% paraformaldehyde in 0.1 M phosphate-buffered saline, pH 7.4, and blocked with 2% heat-inactivated fetal bovine serum/2% bovine serum albumin in phosphate-buffered saline with 0.1% triton-X 100 for 1 h at ~25°C. Antibodies against [microtubule-associated protein (MAP-2) 21 : 6000; Sigma-Aldrich, Oakville, ON, Canada] and VAMP2 (1 : 500; Chemicon) were used in blocking solution overnight at 4°C. Cells were labelled with Alexa 488 or Alexa 546 secondary antibodies (Invitrogen). Analysis of branch complexity was performed on MAP-2 positive processes as described (Sholl 1953). For quantitative measurements of synaptic puncta, we counted the number of VAMP2-immunoreactive pre-synaptic puncta closely apposed to the proximal 30 μm segments of MAP-2-positive primary dendrites. The density of pre-synaptic puncta was calculated by dividing the number of VAMP2-positive puncta by the surface area of the proximal dendritic segments measured. The average density of pre-synaptic puncta was calculated for each embryo and subjected to one-way ANOVA followed by a *post hoc* Tukey test.

Golgi staining and analysis of dendritic spine morphology

Neuronal morphology was analyzed with tissue stained using the Golgi-Cox impregnation technique. Adult wild-type and RPTP$\sigma^{-/-}$ mice were euthanized and brains processed as dictated by the FD Rapid GolgiStain Kit (FD Neurotechnologies, Inc., Columbia, MD, USA). Tissue was sliced into thick horizontal serial 100 μm sections with a cryostat (Leica CM1850; Leica Microsystems Inc., Richmond Hill, ON, Canada).

Spines of primary CA1 dendrites traced by an investigator blind to animal genotype were imaged on a light microscope (Nikon Eclipse E800; Nikon, Melville, NY, USA) with a 100× oil-immersion objective (Nikon, n.a. 1.30), using the Neurolucida 9 program (MBF Bioscience Inc., Williston, VT, USA). Analysis of tracings was performed with the NeuroExplorer 9 program. Student's *t*-test was used to compare the data between genotypes.

Electrophysiological recordings

Field recordings were performed on slices obtained from adult male wild-type and RPTP$\sigma^{-/-}$ mice (8–12 weeks old) as described (Chapman *et al.* 1998; Kourrich and Chapman 2003). Animals were anesthetized with isoflurane and brains removed and cooled (4°C) in oxygenated (95% O_2, 5% CO_2) artificial CSF (ACSF). ACSF consisted of 124 mM NaCl, 2.5 mM KCl, 1.25 mM NaH_2PO_4, 1.3 mM $MgSO_4$, 2.5 mM $CaCl_2$, 26 mM $NaHCO_3$, and 10 mM dextrose (5 mM KCl, 2 mM $MgSO_4$ and 2 mM $CaCl_2$ for plasticity experiments). Acute hippocampal slices (400 μm) were cut using a vibratome (Leica Microsystems, GmbH, Germany) and placed on a nylon net in a gas-fluid interface recording chamber (Fine Science Tools, Foster City, CA, USA) in which oxygenated ACSF was perfused at 1.0–2.0 ml/min at 32°C. Slices were allowed to recover 1 h before recordings.

Field excitatory post-synaptic potential (fEPSP) recordings were obtained using glass micropipettes filled with 2 M NaCl (2 to 5 MΩ) positioned in the middle of stratum radiatum. A bipolar stimulating electrode constructed from 0.1 MΩ tungsten electrodes (Frederick Haer & Co., Bowdoin, ME, USA) was placed in stratum radiatum at least 500 μm from the recording electrode. Constant current stimulation pulses (0.1 ms duration) were delivered using a stimulus isolation unit (WPI, Models A300 and A360). Field potentials were filtered (3 kHz low-pass) and amplified with an AxoClamp 2B amplifier (Molecular Devices, Sunnyvale, CA, USA), and digitized at 20 kHz (Digidata 1322A; Molecular Devices) for storage using Clampex 8.1 software (Molecular Devices). Input–output tests monitored synaptic responses evoked by a range of stimulus intensities in increments between 25 and 200 μA.

Responses to test pulses were monitored every 20 s for at least a 20-min baseline period prior to the induction of LTP or long-term depression (LTD). The intensity of test pulses was adjusted to evoke fEPSPs with an amplitude of 60–70% of the maximum observed during input–output tests. High-frequency stimulation to induce LTP consisted of a 1-s 100 Hz train of pulses (Chapman *et al.* 1998). Low-frequency stimulation used to induce LTD consisted of 900 pairs of pulses (25 ms interpulse interval), delivered at 1 Hz for

15 min (Thiels *et al.* 1996; Kourrich and Chapman 2003). Responses evoked by test pulses were monitored every 20 s following conditioning stimulation.

The rising fEPSP slope was measured using Clampfit software (Molecular Devices). Changes in fEPSPs were assessed using mixed design ANOVAs and Neuman–Keuls tests that compared averaged measures during the baseline period, 1 min after conditioning stimulation, and during the last 20 min of recordings.

Miniature excitatory post-synaptic currents (mEPSCs) were recorded in whole-cell patch-clamp mode from CA1 pyramidal cells using a MultiClamp 700B amplifier (Molecular Devices) in transverse hippocampal slices maintained at 30°C. Recording pipettes (4–5 MΩ) were filled with a solution containing: 100 mM $CsMeSO_3$, 15.5 mM CsCl, 10 mM TEA–Cl, 10 mM HEPES, 0.25 mM EGTA, 8 mM NaCl, 10 mM dextrose, 2 mM MgATP, and 0.4 mM Na_3GTP (pH 7.2–7.3, 280–290 mOsm). Picrotoxin (100 μM) and tetrodotoxin (0.5 μM) were added to the extracellular ACSF prior to recordings. Cells were voltage-clamped at −60 mV and series (10–30 MΩ) and input (100–200 MΩ) resistances were monitored online throughout each experiment. Data acquisition was digitized at 10 kHz and filtered at 2 kHz (Digidata 1440A; Molecular Devices) for storage using pClamp10 software (Molecular Devices). Analysis was performed with MiniAnalysis software (Synaptosoft, Fort Lee, NJ, USA) selecting 100 events at random per cell. Threshold mEPSC amplitude was set at 4 pA.

Novel object recognition test

Recognition memory was assessed using the novel object recognition test (Bevins and Besheer 2006). Briefly, the mice were individually habituated to a brightly lit, empty open field for a period of 10 min. Twenty-four hours later, the mice were returned to the field, but this time the area contained two identical, biologically neutral objects, placed equidistant from the centre and walls of the field. Each mouse was allowed to explore the objects for a period of 5 min, after which the mouse was returned to its cage to rest for 4 h. Following the 4-h rest period, the mouse was returned to the same testing field, but with one of the familiar objects replaced by a similar-sized novel object. The mouse's exploration was tracked for 5 min with an overhead video recorder (VideoTrack; ViewPoint Life Sciences Inc., Montreal, QC, Canada). *Post hoc*, the amount of time that the mouse spent exploring the novel object relative to the amount of time spent exploring the familiar object was used to generate a difference score. Enhanced cognitive performance is measured by an increased exploration of the novel object. Measurements were subjected to statistical analysis using a two-tailed Student's *t*-test.

Results

RPTPσ is enriched in synaptic membranes in mature brain

To identify the possible contribution of RPTPσ to synaptic function, we initially assessed the distribution of RPTPσ in the neocortices of P14 and mature rats using subcellular fractionation. Protein was detected using a monoclonal antibody (17G7.2) that does not bind LAR or RPTPδ and is specific for RPTPσ (Thompson *et al.* 2003). Type IIa RPTPs, including RPTPσ, are transmembrane proteins that are proteolytically processed and presented on the cell surface as non-covalently linked extracellular and intracellular domains (Aicher *et al.* 1997). In homogenates of P14 and adult rat brain, and in subsequent fractions that contain membranes, antibody 17G7.2 detected an approximately 80 kDa band, consistent with the molecular weight of the intracellular domain of RPTPσ. The RPTPσ intracellular domain was abundant in the crude synaptosomal fraction (P2), derived from the neocortices of P14 and mature rats. The P2 fractions were then hypotonically lysed and further separated into fractions enriched for synaptosomal plasma membranes (LP1) and synaptic vesicles (LP2). RPTPσ was enriched in the synaptic plasma membrane (LP1) and vesicle-enriched (LP2) fractions of the neocortices from both P14 and adult rats (Fig. 1). Synaptotagmin and GluR2/3 immunoreactivity illustrate the enrichment of pre-synaptic and post-synaptic markers, respectively.

We then applied a second method that generates fractions enriched with components of the post-synaptic density (PSD) (Fallon *et al.* 2002). Using this technique, synaptophysin was not detected in the PSD fractions, consistent with pre-synaptic proteins fractionating away from the PSD. In contrast, RPTPσ co-fractionated with PSD-95, a major component of the PSD (Fig. 1). These findings indicate that in addition to the previously described role for pre-synaptic RPTPσ promoting synaptogenesis, RPTPσ is also present on the post-synaptic side of developing and mature synapses.

To determine if the absence of RPTPσ altered the expression of the other LAR subfamily members, western blots of whole brain homogenates derived from adult $RPTP\sigma^{+/+}$ and $RPTP\sigma^{-/-}$ mice were probed with antibodies directed against RPTPδ and LAR. No change in the level of expression of either RPTPδ or LAR was detected (Fig. 1).

Increased mossy fiber innervation and axon sprouting in RPTPσ null mice

RPTPσ inhibits axon extension during neural development and axon regeneration in the CNS following injury (Thompson *et al.* 2003; Sapieha *et al.* 2005; Shen *et al.* 2009; Fry *et al.* 2010). We therefore investigated the possibility that RPTPσ expression in the mature CNS might function to restrain axon collateral sprouting. Hippocampal granule cell mossy fibers course through the hilus of the dentate gyrus and normally form a narrow band within the stratum lucidum where they synapse on the dendrites of CA3 pyramidal neurons (Fig. 2a). In the adult brain, mossy fibers sprout collateral branches out of the stratum lucidum into stratum oriens of subregion CA3c during normal aging and in response to pathological conditions, such as seizure (Schopke *et al.* 1991; Cavazos *et al.* 1992; Masukawa *et al.* 1995; Adams *et al.* 1997; Magarinos *et al.* 1997; Teter *et al.* 1999; Ramirez-Amaya *et al.* 2001). Thus, we investigated the possibility that RPTPσ might influence axonal sprouting caused either by aging or due to seizures induced by injection of KA.

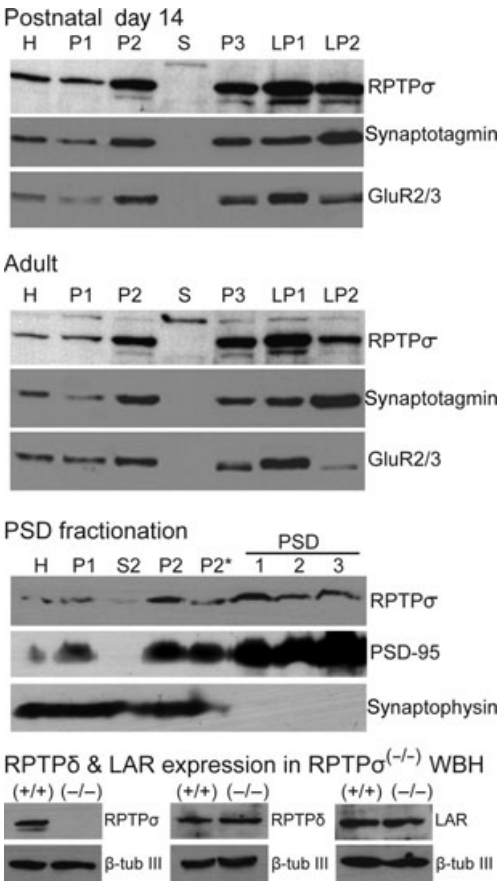

Fig. 1 Fractionation of RPTPσ in postnatal day 14 and mature brain. Subcellular fractionation of postnatal day 14 (P14) and adult rat cortical lysates illustrates that RPTPσ is enriched in the synaptosome fraction (P2) in developing and mature cortices. Hypotonic lysis and further fractionation indicate enrichment of RPTPσ in the synaptosomal membrane fraction (LP1) derived from the cortex of adult and P14 brains. Distributions of synaptotagmin and GluR2/3 illustrate the fractionation of pre-synaptic and post-synaptic markers. Post-synaptic density (PSD) fractionation of adult rat brain reveals co-fractionation of RPTPσ with PSD-95 in the PSD fraction. The pre-synaptic protein synaptophysin was not detected in the PSD fraction. (H: homogenate; of whole cells; P1: nuclei and cellular debris; P2: mitochondria, plasma membrane, synaptosomes, and synaptic vesicles; P2*: plasma membrane, synaptosomes, and synaptic vesicles; S: cytosol and soluble fraction; P3: Golgi apparatus; endoplasmic reticulum, internal membranes; LP1: synaptic plasma membrane; LP2: synaptic vesicles, microsomes; PSD: post-synaptic densities). Whole brain homogenate from RPTP$\sigma^{+/+}$ and RPTP$\sigma^{-/-}$ mice was probed using antibodies directed against the intracellular subunits of LAR subfamily members and no change was detected in expression of RPTPδ and LAR in the absence of RPTPσ. β-tubulin III staining shows equal loading of RPTP$\sigma^{+/+}$ and RPTP$\sigma^{-/-}$ whole brain homogenates.

To evaluate the distribution of mossy fiber axons innervating CA3, we measured the surface area occupied by dark Timm labelling, a histochemical stain that selectively labels mossy fiber axons (Amaral and Dent 1981; Danscher 1981). All of the young adult wild-type ($n = 5$) and RPTP$\sigma^{-/-}$ mice ($n = 6$) developed status epilepticus following i.p. injection of KA, with similar severity between the two genotypes (Table 1, chi-squared test, $p > 0.05$). Prolonged seizure activity can induce neuronal loss in hippocampus and other limbic structures and such damage can contribute to axonal sprouting and circuit reorganization in the epileptic brain (Nadler 2003; Morimoto *et al.* 2004; Sutula 2004). Importantly, certain inbred mouse strains, including the Balb/C genetic background used here, are relatively resistant to KA-induced excitotoxic cell damage and mossy fiber sprouting (Schauwecker and Steward 1997; Cantallops and Routtenberg 2000; McKhann *et al.* 2003). To determine if loss of RPTPσ might affect seizure-related neuronal damage and cell death, which might contribute to mossy fiber sprouting, we carried out an unbiased count of cells within the hilar area. This revealed no increased cell loss in RPTP$\sigma^{-/-}$ mice compared with wild-type littermates following KA-induced seizures, indicating that differences in seizure-induced cell death do not contribute to mossy fiber sprouting (three-way repeated measures ANOVA, $p > 0.05$, Table 2).

We then assessed the density of Timm staining within the CA3a and CA3c subregions of stratum oriens (Fig. 2a) in young untreated, aged untreated, or young KA-treated, RPTP$\sigma^{-/-}$ and wild-type littermate mice. The extent of mossy fiber innervation across the entire surface area of CA3 stratum oriens, measured as the surface area occupied by Timm granules, did not differ significantly between RPTP$\sigma^{-/-}$ and wild-type mice regardless of age or KA-treatment ($p > 0.05$, Fig. 2b). Nor did the optical density within the CA3c or CA3a subregions of stratum oriens differ between young untreated RPTP$\sigma^{-/-}$ and wild-type mice (Fig. 2c and d), indicating that the absence of RPTPσ did not detectably alter the projection of mossy fiber axons to CA3 during early development up to young adulthood. With aging, increased Timm labeling was detected in subregion CA3a, distal to the dentrate gyrus, but this increase did not differ between genotypes (Fig. 2d and e). In contrast, following seizures or in aged animals, the CA3c subregion, proximal to the dentate gyrus, exhibited a signficantly higher density of Timm granules in RPTP$\sigma^{-/-}$ compared with wild-type mice (Fig. 2c and e). These findings reveal that the RPTP$\sigma^{-/-}$ mice exhibit increased mossy fiber axon sprouting in CA3c following KA-induced seizure and as a result of normal aging. We conclude that RPTPσ expression inhibits axon collateral sprouting in the mature CNS.

Increased density of pre-synaptic puncta formed by RPTPσ null cortical neurons *in vitro*

As a first step toward determining whether RPTPσ alters the density of synaptic innervation, cortical neurons were obtained from E15 wild-type and RPTP$\sigma^{-/-}$ littermate mouse embryos and cultured for two weeks *in vitro*. Pre-synaptic

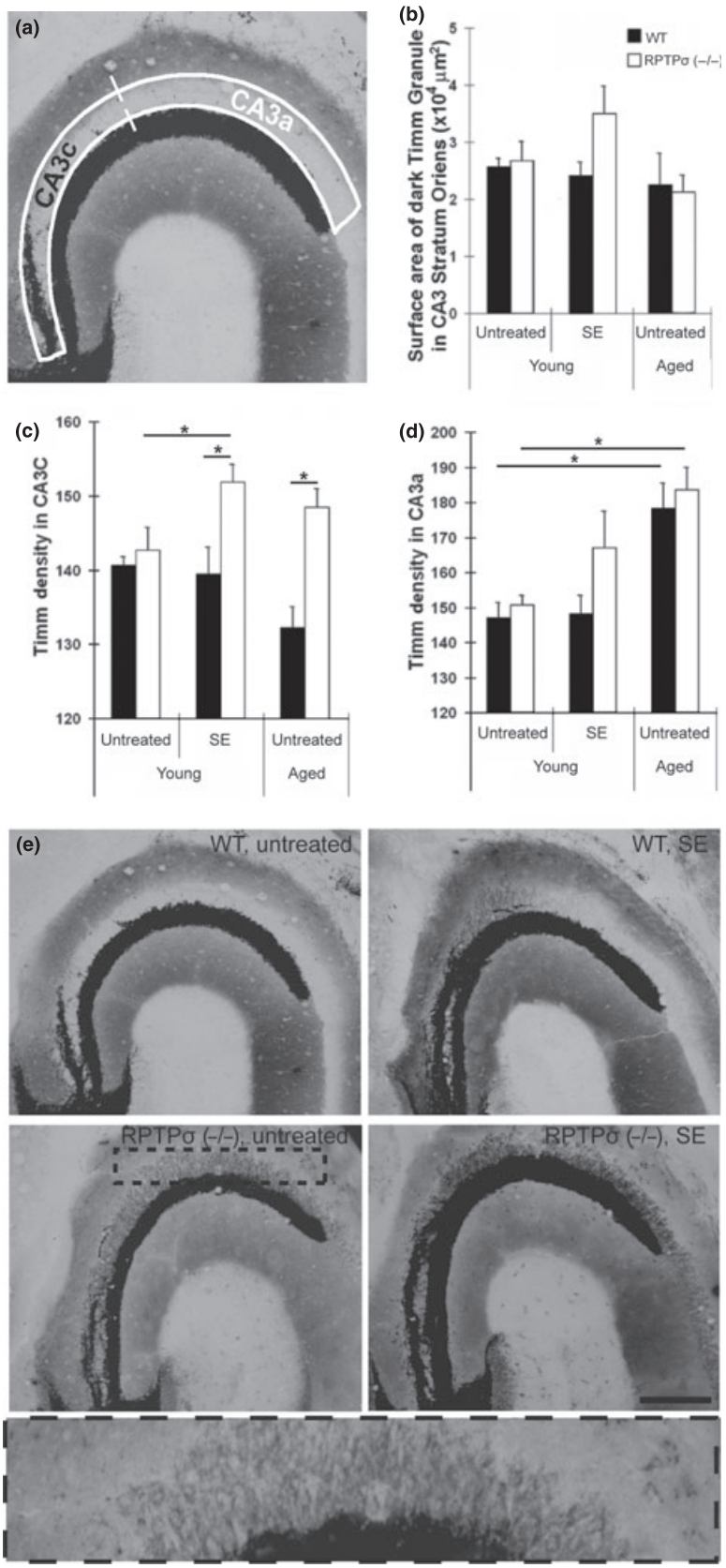

Fig. 2 Increased mossy fiber axon sprouting in CA3c of aged and KA-treated RPTP$\sigma^{-/-}$ mice. (a) Representative image of Timm staining in area CA3. The white contour highlights the region of CA3 stratum oriens measured. The stratum oriens was further divided into two equal size subregions, defined here as CA3c (the subregion proximal to dentate gyrus), and CA3a (the subregion distal to DG). (b) Histogram illustrating quantification of the entire CA3 surface area. Measures were taken from young untreated wild-type, young untreated RPTP$\sigma^{-/-}$, young KA-treated wild-type, young KA-treated RPTP$\sigma^{-/-}$, aged untreated wild-type, and aged untreated RPTP$\sigma^{-/-}$ mice. Although the mean density of Timm staining increased in the KA-treated RPTP$\sigma^{-/-}$ mice, no significant differences in surface area occupied by dark Timm granules over this measure of entire surface area of CA3 were present between genotypes and conditions (three-way repeated measures ANOVA, $p > 0.05$; for genotype effect: young untreated WT vs. KO $p = 0.79$; young KA-treated WT vs. KO $p = 0.08$; old untreated WT vs. KO $p = 0.85$). (c) To assess regionally specific effects on axon sprouting, CA3 was divided into CA3a and CA3c. In the CA3c subregion, proximal to the DG, measurement of optical density revealed that RPTP$\sigma^{-/-}$ mice exhibit significantly more mossy fiber sprouting compared with wild-type mice, in aged animals or following seizure (four-way repeated measures, $^*p < 0.05$). (d) In the CA3a subregion, RPTP$\sigma^{-/-}$ mice do not exhibit more mossy fiber sprouting compared with wild-type mice in the CA3a region, distal to the DG, following seizures. While aging resulted in increased Timm labelling in area CA3a ($^*p < 0.0001$), the difference does not differ between genotypes (young untreated WT vs. KO $p = 0.49$; young KA-treated WT vs. KO $p = 0.14$; old untreated WT vs. KO $p = 0.60$). (e) Representative images of CA3 taken from young wild-type untreated (upper left), aged knockout untreated (lower left), and KA-treated mice (right column). Scale bar: 500 μm, error bars show SEM. A region showing sprouting in aged-untreated RPTP$\sigma^{-/-}$ brain, outlined by a dashed line, is enlarged and shown below the representative images.

Table 1 Kainic acid-induced status epilepticus

Behavioral seizures	RPTPσ (+/+)	RPTPσ (–/–)
Continuous bilateral forelimb clonus with intermittent unilateral rear limb clonus (Racine classification, class 3 and above)	1 (20%)	2 (33%)
Continuous bilateral rear limb clonus, with intermittent loss of gesture controls and falling (Racine classification, class 4 and above)	1 (20%)	1 (17%)
Continuous bilateral rear limb clonus, with intermittent loss of gesture controls and falling and other signs of severe seizures, especially jumping (Racine classification, class 4 and above with jumping)	3 (60%)	2 (33%)
Died during status epilepticus	0	1 (17%)
Total	5	6

Table 2 Average number of hilar cells per section

	RPTPσ (+/+)	RPTPσ (–/–)
Untreated	36.30 ± 4.10	37.23 ± 3.55
KA-induced SE	36.98 ± 3.88	36.38 ± 2.07

varicosities were scored as VAMP2 immunoreactive puncta closely apposed to MAP-2 immunoreactive dendrites (Fig. 3a) and the density of positive puncta quantified along the most proximal 30 μm of secondary dendrites. These measures revealed an approximately 20% increase in the density of VAMP2-positive puncta in cultures of cortical neurons derived from RPTP$\sigma^{-/-}$ mice compared with wild-type mice (ANOVA with *post hoc* Tukey test, $p < 0.05$, Fig. 3b). Western blots of hippocampal homogenates from wild-type and RPTP$\sigma^{-/-}$ adult mice show no apparent differences in VAMP2 protein levels (Fig. 3c), indicating that increases in VAMP2-positive puncta detected in the cultures derived from RPTP$\sigma^{-/-}$ mice do not result from increased VAMP2 expression in RPTPσ knockouts.

To determine whether RPTPσ influences dendritic branching, dendritic arbor complexity was assessed using Sholl

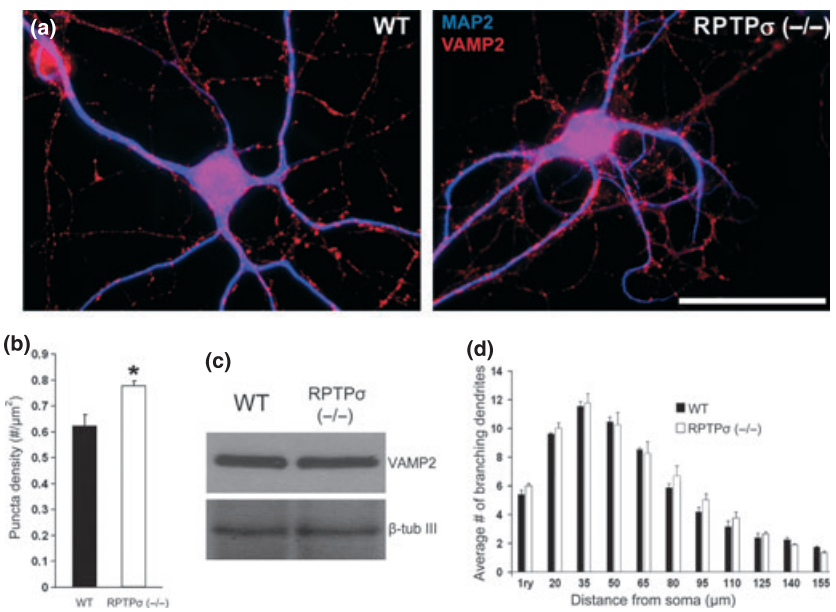

Fig. 3 Increased density of pre-synaptic puncta in cultured cortical neurons from RPTPσ null mice. (a) Immunofluorescence images of cortical neurons, 14 days *in vitro,* derived from wild-type and RPTP$\sigma^{-/-}$ mice labelled with antibodies against MAP-2 (blue) and VAMP2 (red). The density of pre-synaptic specializations was measured by counting the VAMP2-positive varicosities located along proximal MAP-2-positive dendrites. Scale bar: 50 μm. (b) The density of pre-synaptic puncta along proximal dendrites of cortical neurons (within 30 μm of soma) is significantly increased in RPTP$\sigma^{-/-}$ compared with wild-type littermates (Tukey test, $^*p < 0.05$, error bars show SEM). (c) Western blots show no differences in levels of VAMP2 protein in hippocampal homogenates of adult wild-type and RPTP$\sigma^{-/-}$ mice. β-Tubulin III staining shows equal loading of wild-type and RPTP$\sigma^{-/-}$ homogenates. (d) Dendritic branching as measured by Sholl analysis does not differ between genotypes (error bars indicate SEM).

(1953) analysis as described. The number of primary dendrites and branching points at each radius did not differ between genotypes (two-way ANOVA, $p > 0.05$, Fig. 3c), providing evidence that RPTPσ does not affect dendritic branching of cortical neurons *in vitro*.

Increased dendritic spine density and spine length along CA1 pyramidal cell dendrites in RPTPσ null mice

RPTPσ inhibits neurite extension *in vitro* and *in vivo* (Thompson *et al.* 2003; Sapieha *et al.* 2005; Fry *et al.* 2010). Our subcellular fractionation revealed an unexpected enrichment of RPTPσ in PSDs (Fig. 1). The morphology of axonal growth cones and dendritic spines are both highly dependent on the organization of the actin cytoskeleton and similar molecular mechanisms regulate F-actin in both structures (Hotulainen and Hoogenraad 2010; Dent *et al.* 2011). We therefore tested the hypothesis that RPTPσ would inhibit dendritic spine growth and that dendritic spines in mice lacking RPTPσ might be larger than spines in the brains of wild-type littermates. Brains of adult wild-type and RPTP$\sigma^{-/-}$ mice aged from 6 to 7 months were stained using the Golgi-Cox impregnation method. To investigate spine morphology, segments of the primary dendrites of CA1 pyramidal cells (Fig. 4a) were traced to measure the density, length, and diameter of dendritic spines. Consistent with the increased density of pre-synaptic puncta detected *in vitro*, spine density in RPTP$\sigma^{-/-}$ mice was increased relative to wild-type counterparts (Fig. 4b; $n = 44$ dendritic segments per genotype; one-tailed Student's *t*-test, $p < 0.05$). In addition to the increased spine density, we detected a significant increase in the length of dendritic spines in RPTPσ null mice compared with RPTP$\sigma^{+/+}$ mice (Fig. 4b; spines, wild-type: $n = 758$; RPTP$\sigma^{-/-}$: $n = 845$; two-tailed Student's *t*-test, $p < 0.05$). Although this is a modest difference, relatively small changes in dendritic spine geometry are thought to have consequences for synaptic function (Matsuzaki *et al.* 2004; Zito *et al.* 2009). Importantly, the change in morphology detected may result from a mechanistic alteration downstream of RPTPσ that directly regulates dendritic spine elongation, or may be a consequence of a change in synaptic activity due to the absence of RPTPσ, or due to some combination of both.

Altered synaptic properties in hippocampus of RPTPσ null mice

We then assessed the possibility that basal synaptic activity might be sensitive to expression of RPTPσ. We first determined that field potentials evoked by stimulating the Schaffer collaterals and recorded in stratum radiatum of CA1 were similar in acute hippocampal slices from wild-type ($n = 9$) and RPTP$\sigma^{-/-}$ mice ($n = 9$; Fig. 5a). Responses from wild-type and knockout mice did not differ significantly in the magnitude of either the fEPSP amplitude (wild-type: 1.06 ± 1.90 mV; RPTP$\sigma^{-/-}$, 1.07 ± 1.76 mV at 250 μA; $p = 0.98$) or slope (wild-type: 307.64 ± 75.08 μV/ms; RPTP$\sigma^{-/-}$: 320.60 ± 52.64 μV/ms at 250 μA; $p = 0.89$). The absence of RPTPσ therefore does not appear to induce marked changes in extracellular measures of synaptic current in the CA1 region of acute hippocampal slices (Fig. 5b).

We next evaluated if the absence of RPTPσ was associated with functional changes at unitary excitatory synapses. To

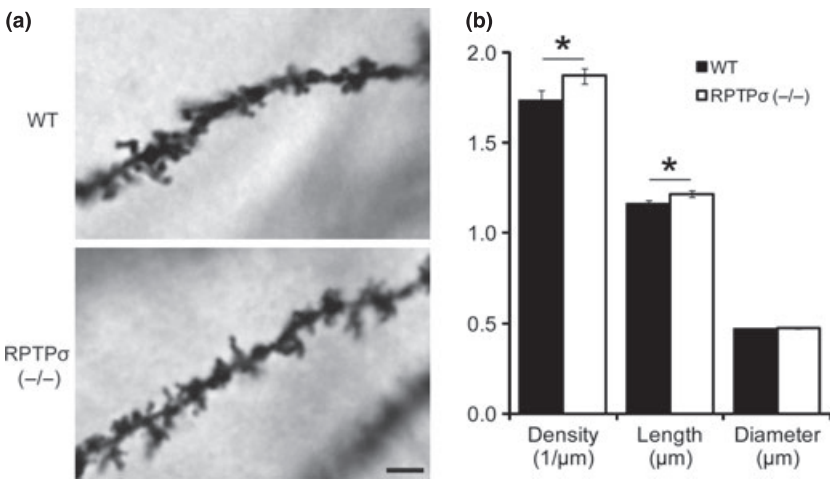

Fig. 4 Increased spine density and length along proximal primary dendrites of CA1 pyramidal cells in RPTP$\sigma^{-/-}$ mice. (a) Representative images of Golgi-Cox stained CA1 pyramidal cell dendrites from adult wild-type and RPTP$\sigma^{-/-}$ mice. Scale bar: 10 μm. (b) RPTP$\sigma^{-/-}$ mice exhibited significantly higher spine density than wild-type mice (4 mice per genotype: for density, $n = 44$ segments/condition (11 dendritic segments of different pyramidal cells per brain, 4 mice per genotype), wild-type: mean = 1.73; RPTP$\sigma^{-/-}$: mean = 1.87; one-tailed Student's *t*-test, $p < 0.05$). When compared with wild-type littermates, a significant increase was detected in the lengths of spines of RPTPσ null mice (wild-type: $n = 758$, mean = 1.16; RPTP$\sigma^{-/-}$: $n = 845$, mean = 1.21; two-tailed Student's *t*-test, $^*p < 0.05$). Error bars indicate SEM.

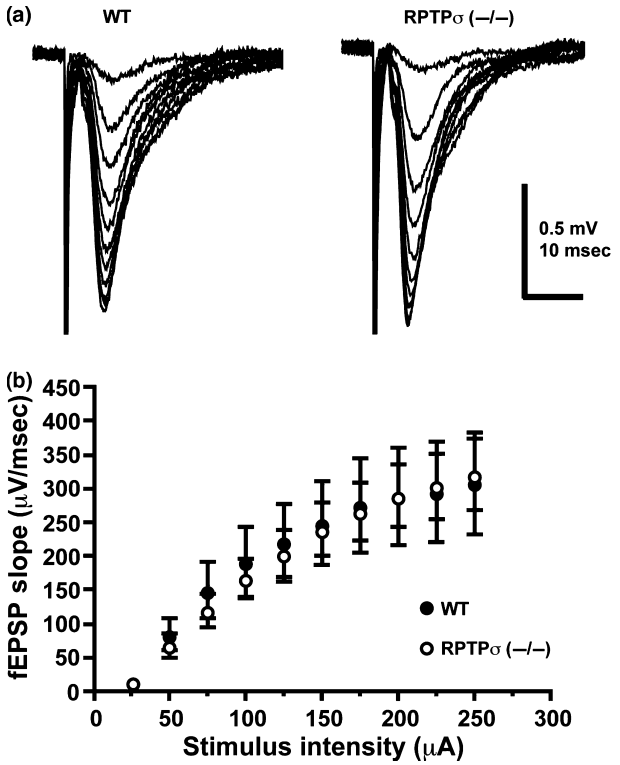

Fig. 5 Similar evoked synaptic field potentials in CA1 in acute hippocampal slices of wild-type and RPTP$\sigma^{-/-}$ mice. (a) Field potentials evoked in CA1 stratum radiatum in acute hippocampal slices by stimulation pulses between 25 and 200 μA are shown for representative slices taken from wild-type and RPTP$\sigma^{-/-}$ mice. (b) Mean input-output curves show the mean slope of the fEPSP as a function of stimulation intensity for each group. Responses did not differ significantly between slices obtained from wild-type animals ($n = 9$) versus RPTPσ knockout mice ($n = 9$). Error bars show SEM.

this end, we recorded miniature AMPAR-mediated excitatory post-synaptic currents (α-amino-3-hydroxy-5-methyl-4-isoxazolepropionic acid mEPSCs) from CA1 pyramidal cells voltage-clamped at -60 mV and compared amplitude, frequency and inter-event interval of spontaneous synaptic events between groups. AMPA mEPSC amplitudes were not significantly different in wild-type and RPTPσ knockout mice (wild-type: 7.51 ± 0.34 pA, $n = 13$; RPTP$\sigma^{-/-}$: 7.25 ± 0.43 pA, $n = 14$; two-tailed Student's t-test; $p = 0.65$) (Fig. 6a and b), suggesting no differences in the maturation state of the synapses. In contrast, the mean frequency of miniature events was increased in CA1 pyramidal cells from RPTPσ knockout mice as compared with wild-type littermates (wild-type: 0.63 ± 0.04 Hz, $n = 11$; RPTP$\sigma^{-/-}$: 0.92 ± 0.09 Hz, $n = 11$; $p < 0.05$) (Fig. 6c). Similarly, the mean inter-event interval was reduced in cells from RPTPσ null mice (wild-type: 1630 ± 102.4 ms, $n = 11$; RPTP$\sigma^{-/-}$: 1188 ± 105.7 ms, $n = 11$; $p < 0.01$) and the cumulative distribution of inter-event intervals in CA1 pyramidal cells from knockout mice was shifted toward shorter intervals relative to cells from wild-type mice (Fig. 6d and e). These data suggest an increase in the total number of AMPAR-bearing synapses in mice lacking RPTPσ.

To further examine the properties of CA1 synapses and determine if the increased number of synapses in RPTPσ null mice was associated with modification of pre-synaptic release probability, we next measured paired-pulse ratios at Schaffer collateral-CA1 synapses. Slices from both wild-type and knockout mice exhibited paired-pulse facilitation at all inter-pulse intervals tested (Fig. 6f), but facilitation tended to be greater in slices from RPTP$\sigma^{-/-}$ mice, with this difference reaching significance at a paired-pulse interval of 50 ms (wild-type: 152.5 ± 3.8%, $n = 13$; RPTP$\sigma^{-/-}$: 165.5 ± 4.7%, $n = 13$; two-way ANOVA followed by a Holm–Sidak's multiple comparison test; $p < 0.05$). This result is consistent with a difference in pre-synaptic release properties, and suggests that the basal probability of release may be lower in RPTPσ null mice than in wild-type littermates.

Having established that RPTP$\sigma^{-/-}$ mice exhibit some differences in their basal synaptic transmission, we subsequently tested the capacity of the Schaffer collateral-CA1 synapses in these slices to undergo long-term potentiation (LTP) and LTD, two widely studied forms of activity-dependent synaptic plasticity (Malenka and Bear 2004). High-frequency stimulation induced LTP of the fEPSP slope in slices from both wild-type ($n = 13$) and RPTP$\sigma^{-/-}$ mice ($n = 15$; Fig. 7a), but the amount of potentiation was reduced in slices from RPTPσ null mice. Immediately following tetanization, responses in slices from RPTP$\sigma^{-/-}$ mice were 160.2 ± 10.5% of baseline as compared with 197.7 ± 13.7% in wild-type slices ($F_{2,52} = 3.32$, $p < 0.05$; Newman–Keuls, $p < 0.01$). This reduced potentiation in slices from RPTPσ null mice persisted after 1 h, at 135.6 ± 7.7% of baseline as compared with 159.9 ± 10.8% in wild-type slices (Newman–Keuls, $p < 0.05$).

Taken together, our findings provide evidence for an increased number of synapses that have a lower probability of release in RPTPσ knockout mice, as reflected by greater mEPSC frequency and by increased paired-pulse facilitation, respectively. These differences in baseline synaptic transmission in RPTP$\sigma^{-/-}$ mice may in part account for their reduced susceptibility to undergo synaptic potentiation in response to high-frequency stimulation. Nevertheless, fEPSPs recorded during a train of high-frequency stimulation (100 Hz for 1 s) did not reveal any obvious differences between wild-type and RPTP$\sigma^{-/-}$ mice.

In contrast to LTP, low-frequency stimulation induced synaptic depression that did not differ significantly between slices from wild-type ($n = 6$) and RPTP$\sigma^{-/-}$ mice ($n = 9$; Fig. 7b). Fifteen minutes of 1 Hz paired-pulse stimulation caused a significant depression of the fEPSP slope immediately after stimulation in both groups (wild-type: 83.9±4.6%; RPTP$\sigma^{-/-}$: 86.6 ± 10.8%; $F_{2,26} = 3.46$, $p < 0.05$; N–K, $p < 0.05$), and the reduction recorded 20–30 min after

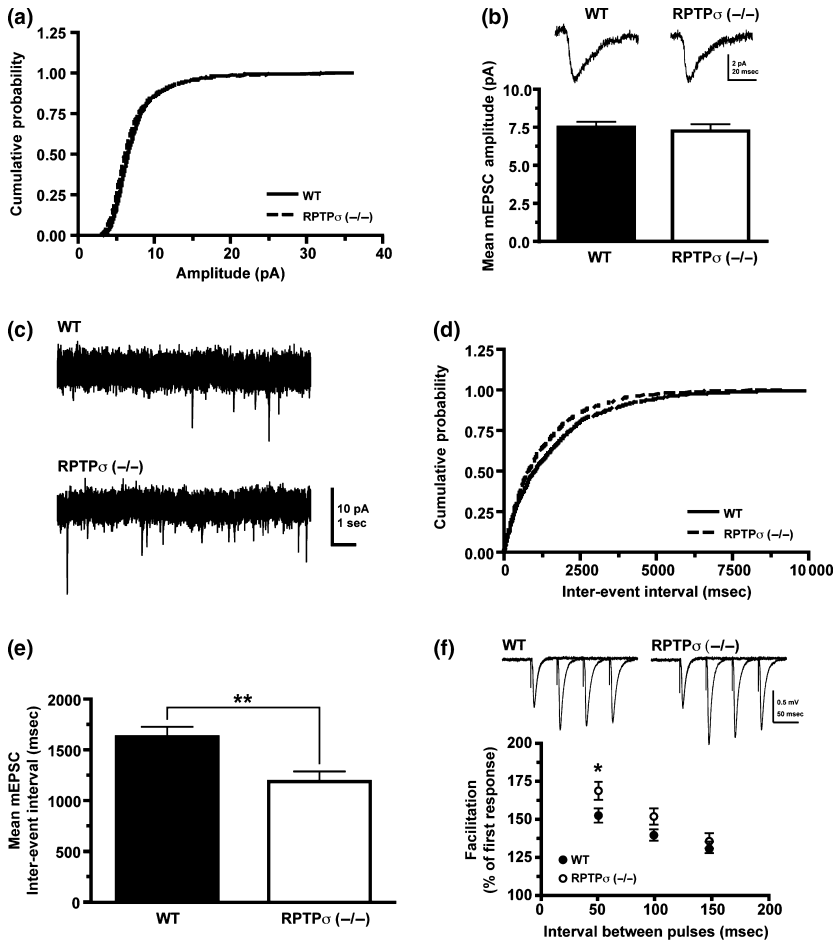

Fig. 6 RPTPσ knockdown does not impact AMPAR mEPSC amplitude but affects AMPAR mEPSC frequency and paired-pulse facilitation. (a) Cumulative plot shows no difference in the amplitudes of AMPA mEPSCs from wild-type and RPTPσ knockout animals. (b) Mean amplitudes per cell are also similar for both groups (wild-type: $n = 13$; RPTP$\sigma^{-/-}$: $n = 14$). (c) AMPA mEPSC frequency is significantly increased in RPTPσ null mice as seen in representative traces. (d) Cumulative plot shows a significant shift towards smaller values for the mean inter-event interval recorded in slices from RPTPσ knockout animals compared with wild-type controls (wild-type: $n = 11$; RPTP$\sigma^{-/-}$: $n = 11$). (e) Mean inter-event interval per cell is also significantly reduced in RPTPσ null mice (two-tailed Student's *t*-test; $^{**}p < 0.01$). (f) Paired-pulse recordings show greater facilitation at 50 ms in slices from RPTPσ knockout animals (wild-type: $n = 13$; RPTP$\sigma^{-/-}$: $n = 13$; two-way ANOVA followed by Holm–Sidak's multiple comparison test; $^{*}p < 0.05$). Sample traces are displayed as an inset above. Error bars indicate SEM.

stimulation did not differ between slices derived from wild-type and RPTP$\sigma^{-/-}$ mice (slope, $F_{2,26} = 0.53$, $p = 0.60$; amplitude, $F_{2,26} = 0.31$, $p = 0.73$).

RPTPσ null mice exhibit enhanced novel object recognition memory

We then assessed recognition memory in these mice using the novel object recognition test (Fig. 8a). This test is considered to evaluate cognition, particularly recognition memory, and is typically applied to rodent models of CNS disorders. Mice exhibit the spontaneous tendency to be more interested in a novel object than a familiar object. The novel object recognition test predicts that if a mouse recalls a familiar object, it will then spend relatively more time exploring a novel object. This test period compares the amount of time that mice spend exploring a novel object with the amount of time spent exploring a familiar object during a 5-min test period (Bevins and Besheer 2006). The difference between the time spent exploring a novel object compared with time spent exploring a familiar object provides a measure of memory for the familiar object. No significant difference in total exploration time was noted between wild-type and RPTP$\sigma^{-/-}$ mice (Fig. 8b; $p = 0.21$, two-tailed Student's *t*-test). Wild-type mice; however, exhibit a relatively low difference score, indicating an intrinsic preference for the familiar object that was chosen for this assay. Comparison of the difference scores of wild-type and RPTP$\sigma^{-/-}$ mice indicates that RPTPσ null mice spend significantly more time than wild-type littermates with the novel object than the familiar object (Fig. 8c; $p < 0.05$, two-tailed Student's *t*-test), providing evidence for enhanced recognition memory in the RPTPσ null mice compared with wild-type littermates.

Discussion

RPTPσ is essential for normal neural development and inhibits axon regeneration following injury, but its function in the intact adult nervous system had not been described. Here, we demonstrate that RPTPσ is enriched at developing and mature synapses. We provide evidence that RPTPσ inhibits axon collateral sprouting and limits synapse formation and the length of dendritic spines in the mature brain. Analyses of synapse function revealed grossly normal basal transmission in mice lacking RPTPσ. However, increases in the mean frequency of AMPAR mEPSCs and in paired-pulse facilitation are consistent with more synapses being made

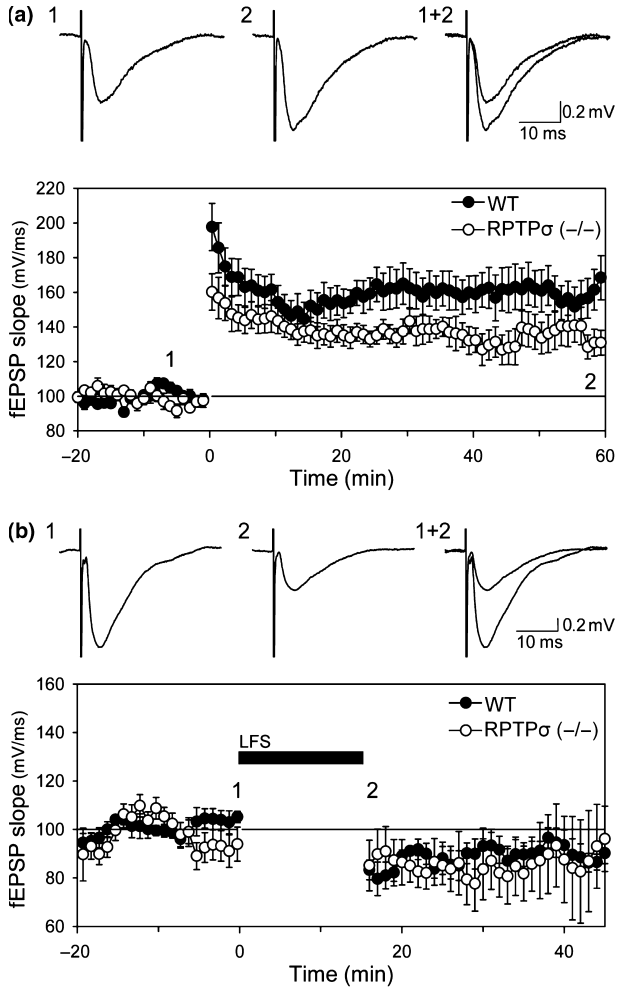

Fig. 7 Reduced long-term potentiation of fEPSPs in RPTPσ null mice. (a) Significantly less potentiation of fEPSPs in slices from RPTP$\sigma^{-/-}$ ($n = 15$) versus wild-type ($n = 13$) animals was measured both immediately and 1 h following high-frequency stimulation (HFS). Traces obtained from an RPTPσ null slice show averaged responses recorded at the end of the baseline period (i) and at the end of the follow-up period (ii). Each point reflects the average of three consecutive responses. (b) Low-frequency paired-pulse stimulation (LFS, bar) induced a transient depression of fEPSP slope in both wild-type and RPTPσ null slices. Traces in b_1 illustrate averaged responses recorded from an RPTP null slice at the end of the baseline period (i) and 1-2 min post-LFS (ii) at the times indicated in B_2. The depression of responses was not significantly different in wild-type ($n = 6$) versus RPTP$\sigma^{-/-}$ ($n = 9$) mice after 30 min. Error bars show SEM.

between neurons lacking RPTPσ and with individual synapses being less effective than wild-type counterparts. Investigating possible contributions of RPTPσ to synaptic plasticity and learning and memory, we show that RPTPσ null mice exhibit reduced LTP and enhanced performance in a novel object recognition task. These findings identify novel contributions of RPTPσ to synaptic structure, function, and plasticity in the mature brain.

RPTPσ, RPTPδ, and LAR share approximately 60% and 85% amino acid identity among their extracellular and intracellular domains respectively (Yan *et al.* 1993). In spite of this level of sequence conservation, functions attributed to RPTPσ often differ from those documented for RPTPδ and LAR. Specifically, RPTPσ expression restrains axon outgrowth during neural development, while RPTPδ and LAR promote axon extension (Wang and Bixby 1999; Thompson *et al.* 2003; Chagnon *et al.* 2004). LAR promotes axon regeneration in the peripheral nervous system (Xie *et al.* 2001), but inhibits regeneration in the CNS (Fisher *et al.* 2011), while RPTPσ inhibits axon regeneration in both the CNS and PNS (McLean *et al.* 2002; Thompson *et al.* 2003; Sapieha *et al.* 2005; Fry *et al.* 2010). Early studies in embryonic chick implicated RPTPσ in promoting axon growth; however, it was not clear at the time if this was due to phosphatase activation or inactivation (Ledig *et al.* 1999; Aricescu *et al.* 2002; Rashid-Doubell *et al.* 2002).

While RPTPσ and LAR bind CSPGs (Shen *et al.* 2009; Fry *et al.* 2010; Coles *et al.* 2011), they also bind heparin sulfate proteoglycans (HSPGs) (Aricescu *et al.* 2002), which in contrast to CSPGs, typically promote axon extension (Van Vactor *et al.* 2006). HSPGs and CSPGs are a heterogeneous group of cell surface and extracellular matrix glycosaminoglycans (Bulow and Hobert 2006). They are widely distributed in the developing and mature CNS, wrapping neuronal cell bodies and synapses in a glycoprotein mesh referred to as the peri-neuronal net, a brain-specific form of extracellular matrix (Frischknecht and Seidenbecher 2008). Among HSPG family members, RPTPσ has been demonstrated to bind agrin and collagen XVIII in vertebrates (Aricescu *et al.* 2002). In *Drosophila*, the HSPGs syndecan and dally-like bind LAR (Fox and Zinn 2005; Johnson *et al.* 2006); however, these HSPGs have distinct functions in the assembly of the visual system (Rawson *et al.* 2005) and at the neuromuscular junction (Johnson *et al.* 2006). Syndecan and dally-like compete to bind LAR, with syndecan activating LAR to promote pre-synaptic terminal growth, and Dally-like inhibition of LAR regulating pre-synaptic active zone structure and synaptic quantal release (Johnson *et al.* 2006).

The differences in function between different LAR family members could result from different responses of the same phosphatase to different ligands, differences in subcellular distribution, or from differences between the specific downstream signaling mechanisms activated by LAR, RPTPσ and RPTPδ. A recent study reported that HSPG binding promotes RPTPσ multimerization, thereby inactivating phosphatase activity, while CSPG binding antagonizes RPTPσ multimerization and promotes phosphatase activation (Coles *et al.* 2011). This supports a mechanism of action whereby the glysosaminoglycan ligand bound determines whether RPTPσ will promote or inhibit motility. Such a mechanism could underlie different responses generated by RPTPσ, RPTPδ and LAR to different ligands.

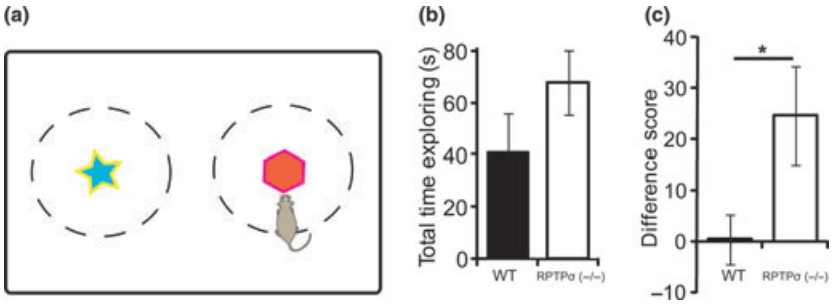

Fig. 8 Enhanced performance in a novel object recognition test by RPTPσ null mice. (a) The novel object recognition test assesses the ability of a mouse to recognize an object that it has already been familiarized with by comparing the amount of time spent exploring a novel object with the amount of time spent exploring a familiar object. The diagram depicts a mouse exploring an object. The mouse must be properly oriented towards the object within the region indicated by the dashed lines for exploration to be scored as positive. (b) Age-matched wild-type and RPTP$\sigma^{-/-}$ mice did not spend significantly different amounts of total time exploring the objects than wild-type littermates (wild-type: $n = 9$; RPTP$\sigma^{-/-}$: $n = 7$; $p > 0.05$ by two-tailed Student's *t*-test; error bars show SEM). (c) The difference score (time spent with novel object minus time spent with familiar object) indicates that RPTP$\sigma^{-/-}$ mice spent significantly more time with the novel object than the familiar object compared with wild-type littermates (*$p < 0.05$ by two-tailed Student's *t*-test; error bars indicate SEM).

Studies carried out *in vitro* indicate that pre-synaptic LAR, RPTPδ, and RPTPσ promote pre-synaptic differentiation of glutamatergic synapses by binding post-synaptic NGL-3 (Woo *et al.* 2009), and in the case of RPTPσ also through interaction with post-synaptic TrkC (Takahashi *et al.* 2011). Our findings provide evidence that loss of RPTPσ function in the mammalian brain reduces synaptic effectiveness while increasing the density of synapses and dendritic spine length *in vivo*, consistent with RPTPσ inhibiting synaptogenesis and dendritic spine growth. Although the identification of an inhibitory role for RPTPσ at synapses may appear at odds with studies indicating that RPTPσ promotes pre-synaptic differentiation, the precise relationship between mechanisms that regulate synapse density and those that promote synaptic differentiation is not clear. Studies investigating potential roles for NGL-3, TrkC, and various glysosaminoglycans interacting with RPTPσ at mature synapses are required.

In addition to the pre-synaptic function of RPTPσ, our findings reveal enrichment in the PSD, supporting a novel role for RPTPσ in dendrites. RPTPσ null mice exhibit elongated dendritic spines, indicating that RPTPσ expression restrains spine growth. RPTPσ activates p250GAP, thereby inhibiting Rac (Chagnon *et al.* 2010), which is a central regulator of dendritic spine morphology (Penzes *et al.* 2008). The RPTPσ binding proteins TrkC and NGL-3 are both localized to post-synaptic specializations (Woo *et al.* 2009; Takahashi *et al.* 2011) and the described trans-synaptic interactions between pre-synaptic RPTPσ and post-synaptic NGL-3 and TrkC likely occur in parallel to RPTPσ localized to the PSD. The specific contribution of dendritic RPTPσ to synaptic differentiation and the pre-synaptic binding partners involved remains to be identified.

Although RPTPσ null mice exhibit a number of morphological abnormalities within the CNS (Elchebly *et al.* 1999; Wallace *et al.* 1999), our electrophysiological findings indicate that they nonetheless present grossly normal basal synaptic transmission. We did, however, detect an increase in the mean frequency of mEPSCs recorded at excitatory synapses, suggesting an increased number of synapses in RPTPσ null mice. This result is consistent with our anatomical findings *in vitro* and *in vivo,* demonstrating that neurons in culture exhibit a higher density of VAMP2-positive puncta, and that CA1 hippocampal pyramidal neurons in RPTPσ knockout mice exhibit a higher density of dendritic spines. Our analysis of paired-pulse ratios suggests that Schaffer collateral synapses onto CA1 neurons in RPTPσ null mice have an abnormally low probability of release. In the neocortex, immature synapses typically show an initial high probability of transmitter release that declines as maturation proceeds (Feldmeyer and Radnikow 2009). Therefore, the low probability of release detected in knockouts could correlate with relatively mature pre-synaptic function in RPTPσ null mice. However, increased AMPA mEPSC amplitude is associated with increased post-synaptic maturity (Hsia *et al.* 1998), yet our mEPSC analysis revealed no differences in the mean amplitude of events recorded in wild-types or RPTPσ null littermates, and therefore does not indicate differences in post-synaptic maturation. Together, these findings support the conclusion that the absence of RPTPσ increases the density of synapses between neurons, but that individual synapses lacking RPTPσ are less effective than wild-type counterparts.

Both RPTPσ and RPTPδ are expressed throughout the hippocampus, however RPTPσ is expressed more widely in the pyramidal cell layer and at more readily detectable levels (Kwon *et al.* 2010). Examining activity-dependent plasticity, we found that RPTPσ null mice have reduced LTP at hippocampal Schaffer collateral-CA1 synapses. Deficits in spatial learning and memory have been documented in RPTPδ null mice (Uetani *et al.* 2000). In contrast, we found

that RPTPσ null mice perform better than wild-type littermates in a novel object recognition test. Interestingly, RPTPδ knockout mice also exhibit a reciprocal disconnection between learning and synaptic plasticity: while Schaffer collateral-CA1 LTP was enhanced in RPTPδ null mice, they have deficits in spatial learning and memory tasks (Uetani *et al.* 2000). These findings reveal that both RPTPσ and RPTPδ contribute to synaptic plasticity and learning and memory, and provide examples in which the ability to induce LTP is not positively correlated with learning and memory capacity. Importantly, this difference between RPTPσ and RPTPδ reveals a previously unappreciated level of functional diversity between members of the type IIa LAR subfamily of tyrosine phosphatases at synapses.

CSPGs exert a potent inhibitory influence on certain forms of synaptic plasticity and learning and memory. For example, enzymatic degradation of CSPGs enhances synaptic plasticity during neural development (Pizzorusso *et al.* 2002), and promotes regeneration, repair and recovery of function in the injured adult CNS (Moon *et al.* 2001; Bradbury *et al.* 2002; Tester and Howland 2008; Garcia-Alias *et al.* 2009). These studies, together with our current findings, suggest that inhibitors of RPTPσ might be developed to manipulate synaptic plasticity, promote recovery of function following injury, and perhaps enhance learning and memory.

Acknowledgements

The authors declare no conflicts of interest. We thank Dr Peter McPherson for providing antibodies. This work was supported by the Canadian Institutes of Health Research (grants 74555, 114965 and 77567). KEH was supported by a Charles Best and Frederick Banting Canada Graduate Scholarship, and BX by a Savoy Foundation Fellowship, JFB is a Fonds de la Recherche en Santé du Québec (FRSQ) Scholar. MLT was supported by the Townshend-Lamarre Foundation and holds the J and J-L Levesque Chair in cancer research. ESR holds a Canada Research Chair and is a Killam Foundation Scholar. CAC was supported by the FRSQ Groupe de Recherche en Neurobiologie Comportementale, the Natural Sciences and Engineering Research Council of Canada, and the Canada Foundation for Innovation. TEK holds a FRSQ Chercheur Nationaux award and is a Killam Foundation Scholar.

References

Adams B., Sazgar M., Osehobo P., Van der Zee C. E., Diamond J., Fahnestock M. and Racine R. J. (1997) Nerve growth factor accelerates seizure development, enhances mossy fiber sprouting, and attenuates seizure-induced decreases in neuronal density in the kindling model of epilepsy. *J. Neurosci.* **17**, 5288–5296.

Aicher B., Lerch M. M., Muller T., Schilling J. and Ullrich A. (1997) Cellular redistribution of protein tyrosine phosphatases LAR and PTPsigma by inducible proteolytic processing. *J. Cell Biol.* **138**, 681–696.

Amaral D. G. and Dent J. A. (1981) Development of the mossy fibers of the dentate gyrus: I. A light and electron microscopic study of the mossy fibers and their expansions. *J. Comp. Neurol.* **195**, 51–86.

Aricescu A. R., McKinnell I. W., Halfter W. and Stoker A. W. (2002) Heparan sulfate proteoglycans are ligands for receptor protein tyrosine phosphatase sigma. *Mol. Cell. Biol.* **22**, 1881–1892.

Bevins R. A. and Besheer J. (2006) Object recognition in rats and mice: a one-trial non-matching-to-sample learning task to study 'recognition memory'. *Nat. Protoc.* **1**, 1306–1311.

Bradbury E. J., Moon L. D., Popat R. J., King V. R., Bennett G. S., Patel P. N., Fawcett J. W. and McMahon S. B. (2002) Chondroitinase ABC promotes functional recovery after spinal cord injury. *Nature* **416**, 636–640.

Bulow H. E. and Hobert O. (2006) The molecular diversity of glycosaminoglycans shapes animal development. *Annu. Rev. Cell Dev. Biol.* **22**, 375–407.

Cantallops I. and Routtenberg A. (2000) Kainic acid induction of mossy fiber sprouting: dependence on mouse strain. *Hippocampus* **10**, 269–273.

Carlin R. K., Grab D. J., Cohen R. S. and Siekevitz P. (1980) Isolation and characterization of postsynaptic densities from various brain regions: enrichment of different types of postsynaptic densities. *J. Cell Biol.* **86**, 831–845.

Cavazos J. E., Golarai G. and Sutula T. P. (1992) Septotemporal variation of the supragranular projection of the mossy fiber pathway in the dentate gyrus of normal and kindled rats. *Hippocampus* **2**, 363–372.

Chagnon M. J., Uetani N. and Tremblay M. L. (2004) Functional significance of the LAR receptor protein tyrosine phosphatase family in development and diseases. *Biochem. Cell Biol.* **82**, 664–675.

Chagnon M. J., Wu C. L., Nakazawa T., Yamamoto T., Noda M., Blanchetot C. and Tremblay M. L. (2010) Receptor tyrosine phosphatase sigma (RPTPsigma) regulates, p250GAP, a novel substrate that attenuates Rac signaling. *Cell. Signal.* **22**, 1626–1633.

Chapman C. A., Trepel C., Ivanco T. L., Froc D. J., Wilson K. and Racine R. J. (1998) Changes in field potentials and membrane currents in rat sensorimotor cortex following repeated tetanization of the corpus callosum in vivo. *Cereb. Cortex* **8**, 730–742.

Cohen R. S., Blomberg F., Berzins K. and Siekevitz P. (1977) The structure of postsynaptic densities isolated from dog cerebral cortex. I. Overall morphology and protein composition. *J. Cell Biol.* **74**, 181–203.

Coles C. H., Shen Y., Tenney A. P., Siebold C., Sutton G. C., Lu W., Gallagher J. T., Jones E. Y., Flanagan J. G. and Aricescu A. R. (2011) Proteoglycan-specific molecular switch for RPTPsigma clustering and neuronal extension. *Science* **332**, 484–488.

Danscher G. (1981) Histochemical demonstration of heavy metals. A revised version of the sulphide silver method suitable for both light and electronmicroscopy. *Histochemistry* **71**, 1–16.

Dent E. W., Gupton S. L. and Gertler F. B. (2011) The growth cone cytoskeleton in axon outgrowth and guidance. *Cold Spring Harb. Perspect. Biol.* **3**, 1–39.

Dunah A. W., Hueske E., Wyszynski M., Hoogenraad C. C., Jaworski J., Pak D. T., Simonetta A., Liu G. and Sheng M. (2005) LAR receptor protein tyrosine phosphatases in the development and maintenance of excitatory synapses. *Nat. Neurosci.* **8**, 458–467.

Elchebly M., Wagner J., Kennedy T. E., Lanctot C., Michaliszyn E., Itie A., Drouin J. and Tremblay M. L. (1999) Neuroendocrine dysplasia in mice lacking protein tyrosine phosphatase sigma. *Nat. Genet.* **21**, 330–333.

Fallon L., Moreau F., Croft B. G., Labib N., Gu W. J. and Fon E. A. (2002) Parkin and CASK/LIN-2 associate via a PDZ-mediated interaction and are co-localized in lipid rafts and postsynaptic densities in brain. *J. Biol. Chem.* **277**, 486–491.

Feldmeyer D. and Radnikow G. (2009) Developmental alterations in the functional properties of excitatory neocortical synapses. *J. Physiol.* **587**, 1889–1896.

Fisher D., Xing B., Dill J. *et al.* (2011) Leukocyte common antigen-related phosphatase is a functional receptor for chondroitin sulfate proteoglycan axon growth inhibitors. *J. Neurosci.* **31**, 14051–14066.

Fox A. N. and Zinn K. (2005) The heparan sulfate proteoglycan syndecan is an in vivo ligand for the Drosophila LAR receptor tyrosine phosphatase. *Curr. Biol.* **15**, 1701–1711.

Frischknecht R. and Seidenbecher C. I. (2008) The crosstalk of hyaluronan-based extracellular matrix and synapses. *Neuron Glia Biol.* **4**, 249–257.

Fry E. J., Chagnon M. J., Lopez-Vales R., Tremblay M. L. and David S. (2010) Corticospinal tract regeneration after spinal cord injury in receptor protein tyrosine phosphatase sigma deficient mice. *Glia* **58**, 423–433.

Garcia-Alias G., Barkhuysen S., Buckle M. and Fawcett J. W. (2009) Chondroitinase ABC treatment opens a window of opportunity for task-specific rehabilitation. *Nat. Neurosci.* **12**, 1145–1151.

Hotulainen P. and Hoogenraad C. C. (2010) Actin in dendritic spines: connecting dynamics to function. *J. Cell Biol.* **189**, 619–629.

Hsia A. Y., Malenka R. C. and Nicoll R. A. (1998) Development of excitatory circuitry in the hippocampus. *J. Neurophysiol.* **79**, 2013–2024.

Johnson K. G., Tenney A. P., Ghose A. *et al.* (2006) The HSPGs Syndecan and Dallylike bind the receptor phosphatase LAR and exert distinct effects on synaptic development. *Neuron* **49**, 517–531.

Kourrich S. and Chapman C. A. (2003) NMDA receptor-dependent long-term synaptic depression in the entorhinal cortex in vitro. *J. Neurophysiol.* **89**, 2112–2119.

Kwon S. K., Woo J., Kim S. Y., Kim H. and Kim E. (2010) Trans-synaptic adhesions between netrin-G ligand-3 (NGL-3) and receptor tyrosine phosphatases lar, PTP{delta}, and PTP{sigma} via specific domains regulate excitatory synapse formation. *J. Biol. Chem.* **285**, 13966–13978.

Ledig M. M., Haj F., Bixby J. L., Stoker A. W. and Mueller B. K. (1999) The receptor tyrosine phosphatase CRYPalpha promotes intraretinal axon growth. *J. Cell Biol.* **147**, 375–388.

Magarinos A. M., Verdugo J. M. and McEwen B. S. (1997) Chronic stress alters synaptic terminal structure in hippocampus. *Proc. Natl Acad. Sci. U. S. A.* **94**, 14002–14008.

Malenka R. C. and Bear M. F. (2004) LTP and LTD: an embarrassment of riches. *Neuron* **44**, 5–21.

Masukawa L. M., O'Connor W. M., Lynott J., Burdette L. J., Uruno K., McGonigle P. and O'Connor M. J. (1995) Longitudinal variation in cell density and mossy fiber reorganization in the dentate gyrus from temporal lobe epileptic patients. *Brain Res.* **678**, 65–75.

Matsuzaki M., Honkura N., Ellis-Davies G. C. and Kasai H. (2004) Structural basis of long-term potentiation in single dendritic spines. *Nature* **429**, 761–766.

McKhann G. M., Wenzel H. J., Robbins C. A., Sosunov A. A. and Schwartzkroin P. A. (2003) Mouse strain differences in kainic acid sensitivity, seizure behavior, mortality, and hippocampal pathology. *Neuroscience* **122**, 551–561.

McLean J., Batt J., Doering L. C., Rotin D. and Bain J. R. (2002) Enhanced rate of nerve regeneration and directional errors after sciatic nerve injury in receptor protein tyrosine phosphatase sigma knock-out mice. *J. Neurosci.* **22**, 5481–5491.

Moon L. D., Asher R. A., Rhodes K. E. and Fawcett J. W. (2001) Regeneration of CNS axons back to their target following treatment of adult rat brain with chondroitinase ABC. *Nat. Neurosci.* **4**, 465–466.

Morimoto K., Fahnestock M. and Racine R'. J. (2004) Kindling and status epilepticus models of epilepsy: rewiring the brain. *Prog. Neurobiol.* **73**, 1–60.

Nadler J. V. (2003) The recurrent mossy fiber pathway of the epileptic brain. *Neurochem. Res.* **28**, 1649–1658.

Penzes P., Cahill M. E., Jones K. A. and Srivastava D. P. (2008) Convergent CaMK and RacGEF signals control dendritic structure and function. *Trends Cell Biol.* **18**, 405–413.

Pizzorusso T., Medini P., Berardi N., Chierzi S., Fawcett J. W. and Maffei L. (2002) Reactivation of ocular dominance plasticity in the adult visual cortex. *Science* **298**, 1248–1251.

Racine R. J. (1972) Modification of seizure activity by electrical stimulation. II. Motor seizure. *Electroencephalogr. Clin. Neurophysiol.* **32**, 281–294.

Ramirez-Amaya V., Balderas I., Sandoval J., Escobar M. L. and Bermudez-Rattoni F. (2001) Spatial long-term memory is related to mossy fiber synaptogenesis. *J. Neurosci.* **21**, 7340–7348.

Rashid-Doubell F., McKinnell I., Aricescu A. R., Sajnani G. and Stoker A. (2002) Chick PTPsigma regulates the targeting of retinal axons within the optic tectum. *J. Neurosci.* **22**, 5024–5033.

Rawson J. M., Dimitroff B., Johnson K. G., Rawson J. M., Ge X., Van V. D. and Selleck S. B. (2005) The heparan sulfate proteoglycans Dally-like and Syndecan have distinct functions in axon guidance and visual-system assembly in Drosophila. *Curr. Biol.* **15**, 833–838.

Sapieha P. S., Duplan L., Uetani N., Joly S., Tremblay M. L., Kennedy T. E. and Di Polo A. (2005) Receptor protein tyrosine phosphatase sigma inhibits axon regrowth in the adult injured CNS. *Mol. Cell. Neurosci.* **28**, 625–635.

Schaapveld R. Q., Schepens J. T., Bachner D., Attema J., Wieringa B., Jap P. H. and Hendriks W. J. (1998) Developmental expression of the cell adhesion molecule-like protein tyrosine phosphatases LAR, RPTPdelta and RPTPsigma in the mouse. *Mech. Dev.* **77**, 59–62.

Schauwecker P. E. and Steward O. (1997) Genetic determinants of susceptibility to excitotoxic cell death: implications for gene targeting approaches. *Proc. Natl Acad. Sci. U. S. A* **94**, 4103–4108.

Schopke R., Wolfer D. P., Lipp H. P. and Leisinger-Trigona M. C. (1991) Swimming navigation and structural variations of the infrapyramidal mossy fibers in the hippocampus of the mouse. *Hippocampus* **1**, 315–328.

Shen Y., Tenney A. P., Busch S. A., Horn K. P., Cuascut F. X., Liu K., He Z., Silver J. and Flanagan J. G. (2009) PTPsigma is a receptor for chondroitin sulfate proteoglycan, an inhibitor of neural regeneration. *Science* **326**, 592–596.

Sholl D. A. (1953) Dendritic organization in the neurons of the visual and motor cortices of the cat. *J. Anat.* **87**, 387–406.

Sommer L., Rao M. and Anderson D. J. (1997) RPTP delta and the novel protein tyrosine phosphatase RPTP psi are expressed in restricted regions of the developing central nervous system. *Dev. Dyn.* **208**, 48–61.

Stryker E. and Johnson K. G. (2007) LAR, liprin alpha and the regulation of active zone morphogenesis. *J. Cell Sci.* **120**, 3723–3728.

Sutula T. P. (2004) Mechanisms of epilepsy progression: current theories and perspectives from neuroplasticity in adulthood and development. *Epilepsy Res.* **60**, 161–171.

Takahashi H., Arstikaitis P., Prasad T., Bartlett T. E., Wang Y. T., Murphy T. H. and Craig A. M. (2011) Postsynaptic TrkC and presynaptic PTPsigma function as a bidirectional excitatory synaptic organizing complex. *Neuron* **69**, 287–303.

Tester N. J. and Howland D. R. (2008) Chondroitinase ABC improves basic and skilled locomotion in spinal cord injured cats. *Exp. Neurol.* **209**, 483–496.

Teter B., Harris-White M. E., Frautschy S. A. and Cole G. M. (1999) Role of apolipoprotein E and estrogen in mossy fiber sprouting in hippocampal slice cultures. *Neuroscience* **91**, 1009–1016.

Thiels E., Xie X., Yeckel M. F., Barrionuevo G. and Berger T. W. (1996) NMDA receptor-dependent LTD in different subfields of hippocampus in vivo and in vitro. *Hippocampus* **6**, 43–51.

Thompson K. M., Uetani N., Manitt C., Elchebly M., Tremblay M. L. and Kennedy T. E. (2003) Receptor protein tyrosine phosphatase sigma inhibits axonal regeneration and the rate of axon extension. *Mol. Cell. Neurosci.* **23**, 681–692.

Tremblay M. L. (2009) The PTP family photo album. *Cell* **136**, 213–214.

Ueda T., Greengard P., Berzins K., Cohen R. S., Blomberg F., Grab D. J. and Siekevitz P. (1979) Subcellular distribution in cerebral cortex of two proteins phosphorylated by a cAMP-dependent protein kinase. *J. Cell Biol.* **83**, 308–319.

Uetani N., Kato K., Ogura H., Mizuno K., Kawano K., Mikoshiba K., Yakura H., Asano M. and Iwakura Y. (2000) Impaired learning with enhanced hippocampal long-term potentiation in PTPdelta-deficient mice. *EMBO J.* **19**, 2775–2785.

Van Vactor D., Wall D. P. and Johnson K. G. (2006) Heparan sulfate proteoglycans and the emergence of neuronal connectivity. *Curr. Opin. Neurobiol.* **16**, 40–51.

Wallace M. J., Batt J., Fladd C. A., Henderson J. T., Skarnes W. and Rotin D. (1999) Neuronal defects and posterior pituitary hypoplasia in mice lacking the receptor tyrosine phosphatase PTPsigma. *Nat. Genet.* **21**, 334–338.

Wang J. and Bixby J. L. (1999) Receptor tyrosine phosphatase-delta is a homophilic, neurite-promoting cell adhesion molecular for CNS neurons. *Mol. Cell. Neurosci.* **14**, 370–384.

Wang H., Yan H., Canoll P. D., Silvennoinen O., Schlessinger J. and Musacchio J. M. (1995) Expression of receptor protein tyrosine phosphatase-sigma (RPTP-sigma) in the nervous system of the developing and adult rat. *J. Neurosci. Res.* **41**, 297–310.

Woo J., Kwon S. K., Choi S., Kim S., Lee J. R., Dunah A. W., Sheng M. and Kim E. (2009) Trans-synaptic adhesion between NGL-3 and LAR regulates the formation of excitatory synapses. *Nat. Neurosci.* **12**, 428–437.

Xie Y., Yeo T. T., Zhang C., Yang T., Tisi M. A., Massa S. M. and Longo F. M. (2001) The leukocyte common antigen-related protein tyrosine phosphatase receptor regulates regenerative neurite outgrowth in vivo. *J. Neurosci.* **21**, 5130–5138.

Xu B., McIntyre D. C., Fahnestock M. and Racine R. J. (2004) Strain differences affect the induction of status epilepticus and seizure-induced morphological changes. *Eur. J. Neurosci.* **20**, 403–418.

Yan H., Grossman A., Wang H., D'Eustachio P., Mossie K., Musacchio J. M., Silvennoinen O. and Schlessinger J. (1993) A novel receptor tyrosine phosphatase-sigma that is highly expressed in the nervous system. *J. Biol. Chem.* **268**, 24880–24886.

Zhang J. S., Honkaniemi J., Yang T., Yeo T. T. and Longo F. M. (1998) LAR tyrosine phosphatase receptor: a developmental isoform is present in neurites and growth cones and its expression is regional- and cell-specific. *Mol. Cell. Neurosci.* **10**, 271–286.

Zito K., Scheuss V., Knott G., Hill T. and Svoboda K. (2009) Rapid functional maturation of nascent dendritic spines. *Neuron* **61**, 247–258.